Scientia Iranica B (2014) 21(2), 387–402

SCIENTIA IRANICA

Sharif University of Technology
Scientia Iranica
Transactions B: Mechanical Engineering
www.scientiairanica.com

Free-edge stresses in general cross-ply laminates

H. Yazdani Sarvestani*

School of Mechanical Engineering, Sharif University of Technology, Tehran, P.O. Box 11155-9567, Iran.

Received 13 September 2012; received in revised form 11 January 2013; accepted 28 September 2013

KEYWORDS
General cross-ply laminate;
Interlaminar stresses;
Elasticity formulation;
First order shear deformation plate theory;
Layerwise theory.

Abstract. Within elasticity theory, the reduced form of a displacement field is obtained for general cross-ply composite laminates subjected to a bending moment. The first-order shear deformation theory of plates and Reddy's layerwise theory are then utilized to determine the global deformation parameters and the local deformation parameters appearing in the displacement fields, respectively. For a special set of boundary conditions an elasticity solution is developed to verify the validity and accuracy of the layerwise theory. Finally, various numerical results are presented within the layerwise theory for edge-effect problems of several cross-ply laminates under the bending moment. The results indicate high stress gradients of interlaminar stress near the edges of laminates.

1. Introduction

With the ever-increasing application of laminated composite, especially in aerospace industries, which require strong, stiff and lightweight structural components, interlaminar stress plays a significant role in the analysis and design of composite structures, since they can lead to catastrophic failure modes like delamination. It has already been shown that the classical lamination theory is incapable of accurately predicting three-dimensional stress states in regions near the edges of laminates known as boundary-layer regions. Because of the substantial importance of boundary-layer phenomenon in practical usage, enormous amounts of research have been undertaken concentrating on the study of interlaminar stress at free edges of composite laminates. Since no exact elasticity solution to this problem is yet known to exist, various approximate analytical and numerical methods have been presented over the past three decades to determine interlaminar stress in the boundary layer.

The most important methods in this area are from the approximate elasticity solutions by Pipes and Pagano [1], the higher-order plate theory by Pagano [2], the boundary layer theory by Tang and Levy [3], the perturbation technique by Hsu and Herakovich [4], finite difference by Pipes and Pagano [5] and finite elements by Wang and Crossman [6] and Whitcomb et al. [7]. A relatively comprehensive discussion of the literature on the interlaminar stress problem is given in a survey paper by Kant and Swaminathan [8]. Investigations into other types of loading have been relatively rare. Tang [9] examined the interlaminar stresses in symmetric angle-ply composite laminates with two simply supported sides and the other two free sides subjected to a uniform lateral load. Using a global high-order shear deformation theory, the modeling and behavior of laminated plates were presented by Lo et al. [10]. They solved the cylindrical bending of angle-ply laminates and simply supported symmetric laminates under pressure on the top surface of the laminates. Because of global displacement assumptions, the transverse strain components are continuous across the interface between dissimilar materials; therefore, transverse stress components are discontinuous at the layer interfaces. This theory is, thus, most often unqualified to obtain the three-dimensional stress field at the ply level. Murthy and Chamis [11],

*. *Tel.: +151 45593832; Fax: +98 2188735688*
E-mail address: hamids.yazdani@gmail.com (H. Yazdani Sarvestani)

utilizing a three-dimensional finite element method, founded interlaminar stresses in composite laminates subjected to various loadings, such as in-plane and out-of-plane shear/bending. Employing the principle of minimum complimentary energy and the force balance method, the analyzing of general unsymmetric laminates under combined in-plane and out-of-plane loads was presented by Kassapoglou [12]. Barbero et al. [13] developed analytical solutions for displacement and stresses in simply supported laminates using the laminate plate theory of Reddy. They supposed constant laminate thickness and neglected the transverse normal stress component in their analysis. Savoia and Reddy [14] employed a displacement separation of variable approaches and the minimization of the total potential energy, and obtained three-dimensional elasticity solutions for antisymmetric angle-ply rectangular laminates under sinusoidal transverse loading. Wu and Kuo [15] predicted interlaminar stresses in composite laminates under cylindrical bending. They used a local higher-order lamination theory. Wu and Yen [16] also utilized a stress mixed finite element method, based on the local high-order lamination theory, to analyze unsymmetrical thick laminated composite plates, which were fully simply supported, subjected to a sinusoidal distribution of transverse load. Kim and Atluri [17] using an approximate method based on equilibrated stress representations and the principle of minimum complementary energy, analyzed interlaminar stresses near straight free edges of beam-type composite laminates under out of planes shear/bending. They included longitudinal degrees of freedom in the stress distributions. They obtained that interlaminar stresses under shear/bending might exhibit substantially different characteristics than those subjected to uniaxial loading or under pure bending. Robbins and Reddy [18] developed a layerwise finite element model of laminated composite plates. They exhibited that their model is capable of computing interlaminar stresses and other localized effects with the same level of accuracy as a conventional three-dimensional finite element model. They examined the bending of simply supported square laminated plates and free edge effects in symmetric angle-ply laminates subjected to axial displacements on the ends. Lee and Chen [19] predicted interlaminar shear stresses by employing a layerwise interlaminar shear stress continuity theory using a layer reduction technique. They considered no thickness stretching in their analysis and obtained only shear transverse stresses. Shu and Soldatos [20] determined stress distributions in angle-ply laminated plates, subjected to cylindrical bending with different sets of edge boundary conditions. Huang et al. [21], using a partially hybrid stress element with interlaminar continuity, analyzed the bending of composite laminated plates. Matsunaga [22] also obtained stress and displacement distributions of simply supported cross-ply laminated composite and sandwich plates subjected to lateral pressure using a global higher-order plate theory. Mittelstedt and Becker [23] utilized Reddy's layerwise laminate plate theory to obtain the closed-form analysis of free-edge effects in layered plates of arbitrary non-orthotropic layups. The approach consists of the subdivision of physical laminate layers into an arbitrary number of mathematical layers through the plate thickness. Jin Na [24] used a finite element model based on the layerwise theory, and von Kármán type nonlinear strains are used to analyze damage in laminated composite beams. In the formulation, the Heaviside step function is employed to express the discontinuous interlaminar displacement field at the delaminated interfaces. Recently, the layerwise theory (LWT) and Improved First-order Shear Deformation Theory (IFSDT) are employed by Nosier and Maleki [25] to analyze free-edge stresses in general composite laminates under extension loads. Kim et al. [26] analyzed interlaminar stresses near free edges in composite laminates by considering interface modeling. This interface modeling provided not only nonsingular stresses but concentrated finite interlaminar stresses, using the principle of complementary virtual work, and the stresses that satisfy the traction-free conditions not only at the free edges but also at the top and bottom surfaces of laminates were obtained. Lee et al. [27] analyzed the interlaminar stresses of a laminated composite patch using a stress-based equivalent single-layer model under a bending load. The adhesive stresses were obtained by solving the equilibrium equations. The authors found that the stress function-based approach was suitable for solving the stress prescribed boundary value problem with accuracy and efficiency, compared to a displacement-based approach, such as the finite element method. Ahn et al. [28] presented an efficient modeling technique using a multi-dimensional method for prediction of free edge stresses in laminate plates. The results obtained by this proposed model were compared with those available in literature. The present models using the p-convergent transition element are demonstrated to be more practical and economical than the previous p-version FEM using only a single element type.

From the literature survey, it appears that, when regarding the failure of structural components because of bending loads, much more often than in-plane loads, little work has been dedicated so far to the development of theoretical or numerical models for predicting the boundary-layer effects of the bending of structural laminates. For this reason, the present study deals with the analytical solution of interlaminar stresses near free edges of a general cross-ply composite laminate subjected to a bending moment. Beginning from the general form of the displacement field for long laminates and making logical hypotheses in joining with the physical behavior of cross-ply laminates, the displacement field is significantly decreased. A layerwise theory (LWT) is utilizing to analyze the bending problem of a general cross-ply laminate with free edges by employing the simplified displacement field. The first-order shear deformation theory is then employed to determine the unknown coefficients in the reduced displacement field. Also, an analytical solution to elasticity equations is developed for a special set of boundary conditions. This solution is employed to exhibit the accuracy of the LWT results.

2. Theoretical formulation

It is intended, here, to determine the interlaminar stresses in a general cross-ply laminate subjected to the bending moment at $x = a$ and $x = -a$. Laminate geometry and coordinate systems are shown in Figure 1. The formulation is limited to linear elastic material behavior and small strain and displacement.

2.1. Elasticity formulation

Here, it is assumed that the laminate is of thickness h, width $2b$, and considered to be long in the x-direction, and loaded at $x = a$ and $x = -a$ only, as shown in Figure 1. Upon integration of the strain-displacement relation, all strain components are a function of y and z only,

The most general form of the displacement field within the kth layer can be shown to be [29]:

$$u_1^{(k)}(x,y,z) = B_4^{(k)}xy + B_6^{(k)}xz + B_2^{(k)}x + u^{(k)}(y,z),$$

$$u_2^{(k)}(x,y,z) = -B_1^{(k)}xz + B_3^{(k)}x - \frac{1}{2}B_4^{(k)}x^2 + \nu^{(k)}(y,z),$$

$$u_3^{(k)}(x,y,z) = B_1^{(k)}xy + B_2^{(k)}x - \frac{1}{2}B_6^{(k)}x^2 + w^{(k)}(y,z), \tag{1}$$

where $u_1^{(k)}(x,y,z)$, $u_2^{(k)}(x,y,z)$ and $u_3^{(k)}(x,y,z)$ are the displacement components in the $x-, y-$, and z-directions, respectively, of a material point initially located at (x,y,z) in the kth ply of the laminate. In order to fulfill the continuity of the displacement at

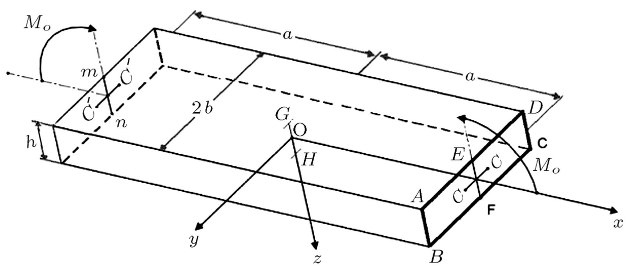

Figure 1. Laminate geometry and coordinate system.

the interface of the layers, it is necessary that the set of constants appearing in Eqs. (1) be the same for all layers within the laminate (i.e. $B_j^{(1)} = B_j^{(2)} = ... = B_j^{(N)} \equiv B_j,\ j = 1, 2, ..., 6$), that is:

$$u_1^{(k)}(x,y,z) = B_4xy + B_6xz + B_2x + u^{(k)}(y,z),$$

$$u_2^{(k)}(x,y,z) = -B_1xz + B_3x - \frac{1}{2}B_4x^2 + \nu^{(k)}(y,z),$$

$$u_3^{(k)}(x,y,z) = B_1xy + B_5x - \frac{1}{2}B_6x^2 + w^{(k)}(y,z). \tag{2}$$

As long as the loading conditions at $x = -a$ and a are similar, based on physical grounds, it is argued here that the following conditions must hold:

$$u_1^{(k)}(x,y,z) = -u_1^{(k)}(-x,-y,z),$$

$$u_2^{(k)}(x,y,z) = -u_2^{(k)}(-x,-y,z),$$

$$u_3^{(k)}(x,y,z) = u_3^{(k)}(-x,-y,z). \tag{3}$$

From Eqs. (2) and (3), it is readily concluded that:

$$u^{(k)}(y,z) = -u^{(k)}(-y,z),$$

$$\nu^{(k)}(y,z) = -\nu^{(k)}(-y,z),$$

$$w^{(k)}(y,z) = w^{(k)}(-y,z), \tag{4}$$

and $B_4 = B_5 = 0$. The displacement in Eq. (2) is, therefore, simplified to what follows:

$$u_1^{(k)}(x,y,z) = B_2x + B_6xz + u^{(k)}(y,z), \tag{5a}$$

$$u_2^{(k)}(x,y,z) = -B_1xz + B_3x + \nu^{(k)}(y,z), \tag{5b}$$

$$u_3^{(k)}(x,y,z) = B_1xy - \frac{1}{2}B_6x^2 + w^{(k)}(y,z). \tag{5c}$$

Next, by replacing $u^{(k)}(y,z)$ by $-B_3y + u^{(k)}(y,z)$ in Eq. (5a), the terms involving B_3 in Eqs. (5a)-(5c) may be neglected since no strains are yielded by such terms. In fact, these terms will correspond to an infinitesimal rigid-body rotation of the laminate about the z-axis in Figure 1. The most general form of the displacement field of the kth layer within an arbitrary laminate is, therefore, reduced to be as:

$$u_1^{(k)}(x,y,z) = B_2x + B_6xz + u^{(k)}(y,z), \tag{6a}$$

$$u_2^{(k)}(x,y,z) = -B_1xz + \nu^{(k)}(y,z), \tag{6b}$$

$$u_3^{(k)}(x,y,z) = B_1xy - \frac{1}{2}B_6x^2 + w^{(k)}(y,z). \tag{6c}$$

For general cross-ply laminates based on physical grounds, the following restrictions will, furthermore, hold (see Figure 1):

$$u_1^{(k)}(-x,y,z) = -u_1^{(k)}(-x,y,z), \tag{7a}$$

$$u_2^{(k)}(x,y,z) = u_2^{(k)}(-x,y,z). \tag{7b}$$

Upon imposing Eq. (7a) on Eq. (6a) it is concluded that $u^{(k)}(y,z) = 0$. Also, from Eqs. (7b) and (6b), it is founded that $B_1 = 0$. Thus, for cross-ply laminates, the most general form of the displacement field is given as:

$$u_1^{(k)}(x,y,z) = B_6xz + B_2x,$$

$$u_2^{(k)}(x,y,z) = \nu^{(k)}(y,z),$$

$$u_3^{(k)}(x,y,z) = -\frac{1}{2}B_6x^2 + w^{(k)}(y,z). \tag{8}$$

It is next noted that if the loading conditions at $x = a$ and $x = -a$ are identical, the following conditions along the line GOH must hold:

$$u_1^{(k)}(x=0,y=0,z) = 0,$$

and:

$$u_2^{(k)}(x=0,y=0,z) = 0. \tag{9}$$

From these conditions it is concluded from Eqs. (8) that $\nu^{(k)}(y=0,z) = 0$ and therefore:

$$u_1^{(k)}(x,y=0,z) = B_6xz + B_2x, \tag{10a}$$

$$u_2^{(k)}(x,y=0,z) = 0. \tag{10b}$$

The second parameter in Relation (10a) indicates that lines, such as AB, EF and DC, within the plan ADCB will remain straight after deformation and, furthermore, B_2 is the uniform axial strain of the laminate in the x-direction due to the bending moment. Denoting the axial displacement of the line EF by a$\bar{L}$ and that of MN by -a$\bar{L}$, it is then concluded that $B_2 = \bar{L}$. The first parameter in Relation (10a), on the other hand, indicates that the plane ADCB rotates about the line cc (in the y direction) and B_6 is the angle of bending γ per unit length.

Denoting the angle of bending of the line EF about line cc by θ, it is, therefore, concluded that $B_6 = \gamma = \frac{\theta}{a}$.

From the preceding discussions, it is evident that either B_2 and B_6 or M_0 must be specified at the ends of the laminate. These conclusions can be arrived by the application of the principle of minimum total potential energy. Substituting the displacement field Eqs. (8) into the linear strain-displacement relations of elasticity [30], the following results will be obtained:

$$\varepsilon_x^{(k)} = B_6z + B_2, \qquad \varepsilon_y^{(k)} = \nu^{(k)}{}_{,y},$$

$$\varepsilon_z^{(k)} = w^{(k)}{}_{,z}, \qquad \gamma_{yz}^{(k)} = \nu^{(k)}{}_{z}, + w^{(k)}{}_{,y},$$

$$\gamma_{xy}^{(k)} = 0, \qquad \gamma_{xz}^{(k)} = 0, \tag{11}$$

where a comma followed by a variable indicates partial differentiation, with respect to that variable. The constitutive relations for the kth orthotropic lamina, with fiber orientations of 0° and 90° only, are given by [31]:

$$\{\sigma\}^{(k)} = [\bar{C}]^{(k)}\{\varepsilon\}^{(k)}, \tag{12}$$

where $[\bar{C}]$ is called the transformed (or off-axis) stiffness matrix. The local equilibrium equations of elasticity are known to be [30]:

$$\sigma_{ij,j} = 0 \qquad i = 1,2,3\ , \tag{13}$$

where body forces are considered to be negligible. Also, the repeated index in Eq. (13) indicates summation from one to three. The displacement equilibrium equations within the kth ply are achieved by substituting Eqs. (11) into Eq. (12) and the subsequent results into Eqs. (10). It is to be noted that the displacement equilibrium equation for $i = 1$ is identically satisfied. Therefore, the results are:

$$\bar{C}_{22}^{(k)}\nu^{(k)}{}_{,yy} + \bar{C}_{44}^{(k)}\nu^{(k)}{}_{,zz} + (\bar{C}_{23}^{(k)} + \bar{C}_{44}^{(k)})w^{(k)}{}_{,yz} = 0,$$

$$(\bar{C}_{44}^{(k)} + \bar{C}_{23}^{(k)})\nu^{(k)}{}_{,zy} + \bar{C}_{44}^{(k)}w^{(k)}{}_{,yy} + \bar{C}_{33}^{(k)}w^{(k)}{}_{,zz}$$

$$= -\bar{C}_{13}^{(k)}B_6. \tag{14}$$

The laminate plate is assumed to have free edges at $y = b$ and $y = -b$; solutions of Eq. (14) must satisfy the following traction-free boundary conditions:

$$\sigma_y^{(k)} = \sigma_{yz}^{(k)} = 0, \quad \text{at} \quad y = \pm b. \tag{15}$$

Unfortunately, however, no analytical solution seems to exist for such a boundary-value problem. For this reason, in the present work, attention is devoted to technical plate theories. It is noted that parameters B_2 and B_6 in Eqs. (8) correspond to the global deformation of the laminate and, therefore, the unknown constants, B_2 and B_6, may be determined from the simple first-order shear deformation plate theory (FSDT). The remaining terms (i.e. $\nu^{(k)}$ and $w^{(k)}$) in Eqs. (8), on the other hand, belong to the local deformations of laminate within the laminate and will be determined by using a layerwise laminated plate theory (LWT).

2.2. First-order shear deformation plate theory

In addition to their inherent simplicity and low computational cost, ESL theories often provide sufficiently accurate illustration of global responses for thin to moderately thick laminates. Among the ESL theories, FSDT, which is also known as the Mindlin-Reissner theory, seems to provide the best compromise as far as solution accuracy and simplicity are involved. The theory assumes that the displacement component of any point within the laminate can be suggested as [32]:

$$u_1(x, yx, z) = u(x, y) + z\Psi_x(x, y),$$

$$u_2(x, y, z) = \nu(x, y) + z\Psi_y(x, y),$$

$$u_3(x, yx, z) = w(x, y). \tag{16a}$$

By comparing Eqs. (16a) with the reduced elasticity displacement field in Eqs. (8), it is concluded that the displacement field of FSDT Eqs. (16a) must have the following simple form:

$$u_1(x, y, z) = B_6 xz + B_2 x,$$

$$u_2(x, yx, z) = \nu(y) + z\Psi_y(y),$$

$$u_3(x, y, z) = -\frac{1}{2}B_6 x^2 + w(y). \tag{16b}$$

By employing the principle of minimum total potential energy [30] and the displacement field in Eqs. (16b), the equilibrium equations within FSDT can be obtained to be as:

$$\delta\nu : N_y' = 0, \tag{17a}$$

$$\delta w : Q_y' = 0, \tag{17b}$$

$$\delta\Psi_y : Q_y - M_y' = 0, \tag{17c}$$

$$\delta B_2 : \int_{-b}^{+b} N_x dy = 0, \tag{18a}$$

$$\delta B_6 : \int_{-b}^{+b} M_x dy - M_0 = 0. \tag{18b}$$

Here, a prime in Eqs. (17) indicates ordinary differentiation, with respect to variable y. Also, at the free edges of the laminate (i.e. at $y = \pm b$), the following boundary conditions must be imposed at these edges:

$$N_y = M_y = Q_y = 0, \quad \text{at} \quad y = \pm b. \tag{19}$$

In Eqs. (17)-(19), the stress and moment resultants are found to be as follows [32]:

$$(M_x, M_y, N_x, N_y, Q_y) = \int_{-h/2}^{h/2} (\sigma_x z, \sigma_y z, \sigma_x, \sigma_y, \sigma_{yz})_{dz}. \tag{20}$$

Based on the displacement field in Eqs. (16b) for general cross-ply laminates, these stress and moment resultants are readily found to be:

$$(N_x, N_y) = (B_{11}, B_{12})B_6 + (A_{11}, A_{12})B_2 + (A_{12}, A_{22})V' + (B_{12}, B_{22})\Psi_y',$$

$$(M_x, M_y) = (D_{11}, D_{12})B_6 + (B_{11}, B_{12})B_2 + (B_{12}, B_{22})V' + (D_{12}, D_{22})\Psi_y',$$

$$Q_y = k_4^2 A_{44}(\Psi_y + W'), \tag{21}$$

where A_{ij}, B_{ij} and D_{ij} are the stretching, bending-stretching coupling and bending stiffness of composite laminates within FSDT [32]. Also, in Eqs. (21), k_4^2 is the shear correction factor introduced in order to improve the accuracy of FSDT. The displacement equilibrium equations are found by substituting Eqs. (21) into Eqs. (17) and (18). Solving these equations under the boundary conditions in Eq. (19) will yield the displacement functions, $\nu(y)$, $\Psi_y(y)$, and $w(y)$ and the unknown constants, B_2 and B_6, which appear in Eq. (16b).

The parameters, B_2 and B_6, which are needed in Eqs. (8), are determined to be:

$$B_6 = \frac{\bar{A}_{11}}{\bar{A}_{11}\bar{D}_{11} - \bar{B}_{11}^2}\frac{M_0}{2b},$$

$$B_2 = -\frac{\bar{B}_{11}}{\bar{A}_{11}\bar{D}_{11} - \bar{B}_{11}^2}\frac{M_0}{2b}. \tag{22}$$

The constant parameters appearing in Eqs. (22) are listed in Appendix A.

In the remainder of the present investigation, the following loading cases will be considered:

Loading case 1:

$$B_2 = -\frac{\bar{B}_{11}}{\bar{A}_{11}\bar{D}_{11} - \bar{B}_{11}^2}\frac{M_0}{2b} = \bar{L}, \quad \text{and}$$

$$B_6 = \frac{\bar{A}_{11}}{\bar{A}_{11}\bar{D}_{11} - \bar{B}_{11}^2}\frac{M_0}{2b}. \tag{23}$$

Loading case 2:

$$B_2 = -\frac{\bar{B}_{11}}{\bar{A}_{11}\bar{D}_{11} - \bar{B}_{11}^2}\frac{M_0}{2b} = \bar{L}, \quad \text{and}$$

$$B_6 = 0. \tag{24}$$

In both cases, the specimen is stretched due to the bending moment. In the first loading case, the cross-ply laminate is allowed to freely rotate about the y-axis, but, in the second loading case, the rotation about the y-axis is restricted (consider the specimen whose lower and upper surfaces parallel to XY are fixed between two jaws, thus, the specimen can stretch in the x direction, but cannot freely rotate about the y-axis. In this form, the specimen is subjected to the bending moment at its two edges).

2.3. Layerwise laminated plate theory of Reddy

Due to the existence of a local high stress gradient and the three-dimensional nature of the boundary-layer phenomenon, the interlaminar stresses in the boundary-layer region cannot be determined accurately by the FSDT theory. Thus, Reddy's layerwise theory, which is capable of modeling localized three dimensional effects, is employed here to carry out the bending interlaminar stress analysis in general cross-ply laminates with free edges. Based on the results in Eqs. (8), obtained within the elasticity formulation, the appropriate displacement field within LWT will be simplified to be:

$$u_1(x,y,z) = B_6xz + B_2x,$$

$$u_2(x,y,z) = V_k(y)\phi_k(z), \quad k = 1,2,...,N+1,$$

$$u_3(x,y,z) = -\frac{1}{2}B_6x^2 + W_k(y)\phi_k(z). \tag{25}$$

In Eqs. (25), u_1, u_2 and u_3 represent the displacement components in the x, y and z directions, respectively, of a material point initially located at (x,y,z) in the undeformed laminate. Also, B_2x, B_6xz and $-\frac{1}{2}B_6x^2$ denote global terms that signify the general behavior of the laminate, and $V_k(y)$ and $W_k(y)(k = 1,2,...,N+1)$ represent the local displacement components of all points located on the kth surface in the undeformed state [32,33]. In Relation (25), N marks the total number of numerical layers considered in a laminate. Furthermore, $\phi_k(z)$ is the global Lagrangian interpolation function that is used for discretization of the displacement through the thickness, and can have linear, quadratic or higher-order polynomial variations of the thickness coordinate z [32]. This way, the displacement components will be continuous through the laminate, but the transverse strain components will not be continuous at the interfaces between adjoining layers. This leaves the possibility of continuous transverse stresses at interfaces separating dissimilar materials. It is to be noted that the accuracy of LWT can be enhanced by subdividing each physical layer into a finite number of numerical layers. Clearly, as the number of subdivisions through the thickness is increased, the number of governing equations and the accuracy of the results are increased. The linear global interpolation function, $\phi_k(z)$, is defined as:

$$\phi_k(z) = \begin{cases} 0 & z \le z_{k-1} \\ \Psi^2_{k-1}(z) & z_{k-1} \le z \le z_k \\ \Psi^1_k(z) & z_k \le z \le z_{k+1} \\ 0 & z \ge z_{k+1} \end{cases}$$

$$(k = 1,2,...,N+1), \tag{26}$$

where $\Psi^j_k(j = 1,2)$ are the local Lagrangian linear interpolation functions within the kth layer, which are defined as:

$$\Psi^1_k(z) = \frac{1}{h_k}(z_{k+1} - z),$$

and:

$$\Psi^2_k(z) = \frac{1}{h_k}(z - z_k), \tag{27}$$

with, h_k being the thickness of the kth layer. Substituting Eqs. (25) into the linear strain-displacement relations of elasticity [30], the results are obtained as:

$$\varepsilon_x = B_6z + B_2, \quad \varepsilon_y = V'_k\phi_k, \quad \varepsilon_z = W_k\phi'_k,$$

$$\gamma_{yz} = V_k\phi'_k + W'_k\phi_k, \quad \gamma_{xz} = 0, \quad \gamma_{xy} = 0. \tag{28}$$

By utilizing the principle of minimum total potential energy, the equilibrium equations within LWT are found. The results are $2(N+1)$ local equilibrium equations corresponding to $2(N+1)$ unknowns, V_k and W_k; and two global equilibrium equations corresponding to B_2 and B_6 can be shown to be:

$$\delta V_k : Q^k_y - \frac{dM^k_y}{dy} = 0, \quad k = 1,2,...,N+1, \tag{29a}$$

$$\delta W_k : Q^k_y - \frac{dM^k_y}{dy} = 0 \quad k = 1,2,...,N+1, \tag{29b}$$

$$\delta B_2 : \int_{-b}^{b} N_x dy = 0, \tag{29c}$$

$$\delta B_6 : \int_{-b}^{b} M_x dy - M_0 = 0. \tag{29d}$$

Also, the boundary conditions at the edges parallel to the x-axis (i.e., at $y = -b, b$) involve the specifications of either V_k of M^k_y and W_k of R^k_y. The generalized stress resultants in Eqs. (29) are defined as:

$$(M^k_y, R^k_y) = \int_{-h/2}^{h/2} (\sigma_y, \sigma_{yz})\phi_k dz,$$

$$(N^k_z, Q^k_y) = \int_{-h/2}^{h/2} (\sigma_z, \sigma_{yz})\phi'_k dz,$$

$$(M_x, N_x) = \int_{-h/2}^{h/2} (\sigma_x z, \sigma_x) dz. \tag{30}$$

The generalized stress resultants in Eqs. (30) are expressed in terms of the unknown displacement functions by substituting Eqs. (28) into Eq. (12) and the subsequent results into Eqs. (30). The results are obtained, which can be represented as:

$$\begin{aligned}(M_x^k, N_x^k, M_y^k, N_z^k) =&(D_{11}, B_{11}, D_{12}^k, \bar{B}_{13}^k)B_6\\ &+ (B_{11}, A_{11}, B_{12}^k, A_{13}^k)B_2\\ &(D_{12}^k, B_{12}^k, D_{22}^{kj}, B_{23}^{jk})V_j'\\ &+ (\bar{B}_{13}^k, A_{13}^k, B_{23}^{kj}, A_{33}^{kj})W_j,\end{aligned}$$

$$(R_y^k, Q_y^k) = (B_{44}^{kj}, A_{44}^{kj})V_j + (D_{44}^{kj}, B_{44}^{jk})W_j', \tag{31}$$

where in Eqs. (31), the laminate rigidities are defined as:

$$(A_{pq}^{kj}, B_{pq}^{kj}, D_{pq}^{kj}) = \sum_{i=1}^{N} \int_{-h/2}^{h/2} \bar{C}_{pq}^{(i)}(\phi_k'\phi_j', \phi_k\phi_j', \phi_k\phi_j)dz,$$

$$(A_{pq}^k, B_{pq}^k, \bar{B}_{pq}^k, D_{pd}^k) = \sum_{i=1}^{N} \int_{-h/2}^{h/2} \bar{C}_{pq}^{(i)}(\phi_k', \phi_k, \phi_k' z, \phi_k z)dz,$$

$$(k, j = 1, 2, ..., N+1). \tag{32}$$

The integrations in Eqs. (32) carry out the final expressions of rigidities, which are for convenience, and presented in Appendix B. The local equilibrium equations are expressed in terms of the displacement functions by substituting Eqs. (31) into Eqs. (29a) and (29b). The results are:

$$\begin{aligned}&\delta V_k : A_{44}^{kj}V_j - D_{22}^{kj}V_j'' + (B_{44}^{jk} - B_{23}^{kj})W_j' = 0\\ &\quad k = 1, 2, ..., N+1,\\ &\delta W_k : A_{33}^{kj}W_j - D_{44}^{kj}W_j'' + (B_{23}^{jk} - B_{44}^{kj})V_j'\\ &\qquad = -\bar{B}_{13}^k B_6 - A_{13}^k B_2 \quad k = 1, 2, ..., N+1.\end{aligned} \tag{33}$$

Finally, by substituting Eq. (12) into Eqs. (29c) and (29d), the global equilibrium conditions are expressed in terms of the displacement functions in the following form:

$$\delta B_2 : B_{11}B_6 + A_{11}B_2 + \frac{B_{12}^k}{b}V_k(b) + \frac{A_{13}^k}{2b}\int_{-b}^{b} W_k dy = 0,$$

$$\begin{aligned}\delta B_6 :& D_{11}B_6 + B_{11}B_2 + \frac{D_{12}^k}{b}V_k(b)\\ &+ \frac{\bar{B}_{13}^k}{2b}\int_{-b}^{b} W_k dy = \frac{M_0}{2b}.\end{aligned} \tag{34}$$

3. Analytical solution

In this section, the procedures for solving the displacement equations of equilibrium within LWT and elasticity theory are debated for the cross-ply laminate subject to the bending moment, M_0.

3.1. LWT solution

The system of equations appearing in Eqs. (33) presents $2(N+1)$ coupled second-order ordinary differential equations with constant coefficients, which may be introduced in a matrix form as:

$$[M]\{\eta''\} + [K]\{\eta\} = [T]\{B\}.y, \tag{35}$$

where:

$$\begin{aligned}&\{\eta\} = \left\{\{V\}^T, \{\overline{W}\}^T\right\}^T,\\ &\{V\} = \{V_1, V_2, ..., V_{N+1}\}^T,\\ &\{\bar{W}\} = \{\bar{W}_1, \bar{W}_2, ..., \bar{W}_{N+1}\}^T,\\ &\{B\} = \{B_2, B_6\}^T,\end{aligned} \tag{36a}$$

and:

$$\overline{W}_j = \int^{y} W_j dy. \tag{36b}$$

The coefficient matrices, $[M]$, $[K]$ and $[T]$, are in Eq. (35) and are listed in Appendix B. The general solution of Eq. (35) may be written as:

$$\{\eta\} = [\Psi][\sin h(\lambda y)]\{H\} + [K]^{-1}[T]\{B\}.y, \tag{37}$$

where $[\sin h(\lambda y)]$ is a $2(N+1) \times 2(N+1)$ diagonal matrix. Also, $[\Psi]$ and $(\lambda_1^2, \lambda_2^2, ..., \lambda_{2(N+1)}^2)$ are the modal matrix and eigenvalues of $(-[M]^{-1}[K])$, respectively. In addition, $\{H\}$ is an unknown vector containing $2(N+1)$ integration constants. In the present study, it is assumed that the boundary conditions of the laminate at $y = b$ and $y = -b$ are same. Here, the edges at $y = \pm b$ are free, the following traction-free boundary conditions must be imposed within LWT:

$$M_y^k = R_y^k = 0 \qquad \text{at} \quad y = \pm b. \tag{38}$$

It is to be noted that the unknown, B_2 and B_6, may be found by two different approaches. If B_2 and B_6, are assumed available from FSDT, by satisfying the boundary condition in Eq. (38), the integration constants being in $\{H\}$ will be determined and the problem is solved completely. On the other hand, LWT analysis may be employed to compute the constants, B_2 and B_6. This is readily accomplished with the boundary conditions in Eq. (38) that are first imposed to yield vector in terms of the unknown parameters, B_2 and B_6. These constants are next obtained in terms of the specified bending moment, M_0, by the satisfaction of the global equilibrium condition in Eqs. (34). It should be noted that the analysis within LWT will also be followed for comparing the significance of FSDT in accurate determination of the unknown parameters, b_2 and B_6.

3.2. Elasticity solution

As previously mentioned, no analytical solution seems to exist for Eq. (14) subject to the traction-free boundary conditions in Eq. (15). It is, however, noted here that if the bending rotation is impeded by the end grips (i.e., $B_6 = 0$), while the laminate is being extended in the x-direction, then it is possible to determine an analytical solution for Eq. (14) for the following boundary conditions:

$$\sigma_y^{(k)} = u_3^{(k)} = 0, \quad \text{at} \quad y = \pm b. \tag{39}$$

Such an analytical solution is developed here only to appraise the accuracy of the layerwise theory. With $B_6 = 0$, the displacement field in Eqs. (8) is reduced to:

$$u_1^{(k)}(x,y,z) = -\frac{\bar{B}_{11}}{\bar{A}_{11}\bar{D}_{11} - \bar{B}_{11}^2}\frac{M_0}{2b}x \equiv \bar{L}x,$$
$$u_2^{(k)}(x,y,z) = \nu^{(k)}(y,z),$$
$$u_3^{(k)}(x,y,a) = w^{(k)}(y,z). \tag{40}$$

Also, the elasticity equilibrium equations in Eqs. (14) are simplified into what follows:

$$\bar{C}_{22}^{(k)}\nu^{(k)}{}_{,yy} + \bar{C}_{44}^{(k)}\nu^{(k)}{}_{,zz} + (\bar{C}_{23}^{(k)} + \bar{C}_{44}^{(k)})w^{(k)}{}_{,yz} = 0,$$
$$(\bar{C}_{44}^{(k)} + \bar{C}_{23}^{(k)})v^{(k)}{}_{,yz} + \bar{C}_{44}^{(k)}w^{(k)}{}_{,yy} + \bar{C}_{33}^{(k)}w^{(k)}{}_{,zz} = 0. \tag{41}$$

In terms of the displacement functions appearing in Eqs. (40), the following conditions in Eq. (39) will be given as:

$$w^{(k)}(y,z) = 0,$$
$$\bar{C}_{12}^{(k)}L + \bar{C}_{22}^{(k)}\nu^{(k)}{}_{,y} + \bar{C}_{23}^{(k)}w^{(k)}{}_{,z} = 0 \quad \text{at} \quad y = \pm b. \tag{42}$$

Next, within any layer, it is assumed that:

$$\nu^{(k)}(y,z) = V^{(k)}(y,z) + \bar{\nu}^{(k)}(y),$$
$$w^{(k)}(y,z) = W^{(k)}(y,z) + \bar{w}^{(k)}(y). \tag{43}$$

Upon substituting Eq. (43) into the governing equations of equilibrium (41), two set of equations will be obtained. The first contains $\bar{\nu}^{(k)}$ and $\bar{w}^{(k)}$, as follows:

$$\bar{C}_{22}^{(k)}\bar{\nu}_{,yy}^{(k)} = 0,$$
$$\bar{C}_{44}^{(k)}\bar{w}_{,yy}^{(k)} = 0. \tag{44}$$

The second set of equations contains $V^{(k)}$ and $W^{(k)}$ as:

$$\bar{C}_{22}^{(k)}V^{(k)}{}_{,yy} + \bar{C}_{44}^{(k)}\bar{V}_{,zz}^{(k)} + (\bar{C}_{23}^{(k)} + \bar{C}_{44}^{(k)})W^{(k)}{}_{,yz} = 0,$$
$$(\bar{C}_{44}^{(k)} + \bar{C}_{23}^{(k)})V^{(k)}{}_{,yz} + \bar{C}_{44}^{(k)}W_{,yy}^{(k)} + \bar{C}_{33}^{(k)}W^{(k)}{}_{,zz} = 0. \tag{45}$$

Similarly, substitution of Eq. (43) into the relevant boundary conditions, Eq. (42), at $y = -b$ and $y = b$, yields:

$$\bar{w}^{(k)}(y) = 0,$$
$$\bar{C}_{22}^{(k)}\bar{\nu}_{,y}^{(k)} + \bar{C}_{12}^{(k)}\bar{L} = 0, \tag{46}$$

and:

$$W^{(k)}(y) = 0,$$
$$\bar{C}_{22}^{(k)}V^{(k)}{}_{,y} + \bar{C}_{23}^{(k)}W^{(k)}{}_{,z} = 0. \tag{47}$$

Next, it is noted, from the solutions of the ordinary differential equations in Eqs. (44) and the boundary conditions in Eqs. (46), that it can be concluded:

$$\bar{\nu}^{(k)} = -\frac{\bar{C}_{12}^{(k)}}{\bar{C}_{22}^{(k)}}\bar{L}y = \frac{\bar{C}_{12}^{(k)}}{\bar{C}_{22}^{(k)}}\frac{\bar{B}_{11}}{\bar{A}_{11}\bar{D}_{11} - \bar{B}_{11}^2}\frac{M_0}{2b}y,$$
$$\bar{w}^{(k)} = 0. \tag{48}$$

It remains to solve Eqs. (45) with the boundary conditions in (47). It is noted that the boundary conditions in Eqs. (47) are identically satisfied by assuming the following solution representations:

$$V^{(k)}(y,z) = \sum_{m=0}^{\infty} V_m^{(k)}(z)\sin(\alpha_m y) + V_0^{(k)}(z),$$
$$W^{(k)}(y,z) = \sum_{m=0}^{\infty} W_m^{(k)}(z)\cos(\alpha_m y), \tag{49}$$

where $\alpha_m = (2m+1)\frac{\pi}{2b}$.

Next, upon substitution of Eqs. (49) into Eqs. (45), two sets of ordinary differential equations are obtained as:

$$V_0^{(k)''}(z) = 0, \tag{50}$$

and:

$$-\alpha_m^2 \bar{C}_{22}^{(k)} V_m^{(k)}(z) + \bar{C}_{44}^{(k)} V_m^{(k)''}(z) - \alpha_m (\bar{C}_{23}^{(k)} + \bar{C}_{44}^{(k)}) W_m^{(k)'} = 0,$$

$$\alpha_m (\bar{C}_{44}^{(k)} + \bar{C}_{23}^{(k)}) V_m^{(k)'}(z) - \alpha_m^2 (\bar{C}_{44}^{(k)} W_m^{(k)} + \bar{C}_{33}^{(k)} W_m^{(k)''} = 0. \tag{51}$$

Eq. (50) has the following solution:

$$V_0^{(k)}(z) = E_k z + F_k, \tag{52}$$

where E_k and F_k are unknown constants introduced in the remainder of the present work. Next, in order to solve Eqs. (51), it is assumed that:

$$V_m^{(k)}(z) = B_{km} e^{\lambda_{km} z},$$

$$W_m^{(k)}(z) = C_{km} e^{\lambda_{km} z}. \tag{53}$$

This upon substitution into Eqs. (51) yields the following algebraic equations:

$$\begin{bmatrix} -\alpha_m^2 \bar{C}_{22}^{(k)} + \lambda_{km}^2 \bar{C}_{44}^{(k)} & -\alpha_m \lambda_{km} (\bar{C}_{23}^{(k)} + \bar{C}_{44}^{(k)}) \\ -\alpha_m \lambda_{km} (\bar{C}_{44}^{(k)} + \bar{C}_{23}^{(k)}) & \alpha_m^2 \bar{C}_{44}^{(k)} + \lambda_{km}^2 \bar{C}_{33}^{(k)} \end{bmatrix} \begin{Bmatrix} B_{km} \\ C_{km} \end{Bmatrix} = \begin{Bmatrix} 0 \\ 0 \end{Bmatrix}. \tag{54}$$

For a nontrivial solution, the determinant of the coefficient matrix in Eq. (54) must vanish. This way, a 4th-order polynomial equation in λ_{km} is obtained as follows:

$$\left[\bar{C}_{33}^{(k)} \bar{C}_{44}^{(k)}\right] \lambda_{km}^4 + \alpha_m^2 \left[(\bar{C}_{44}^{(k)} + \bar{C}_{44}^{(k)^2}) - \bar{C}_{22}^{(k)^2} - \bar{C}_{33}^{(k)} \bar{C}_{33}^{(k)} \lambda_{km}^2 + \alpha_m^4 \bar{C}_{22}^{(k)} - \bar{C}_{44}^{(k)} = 0. \tag{55}$$

Eq. (55) has four distinct roots, which may, in general, be complex. Therefore, the general solutions of Eqs. (51) may be presented as:

$$V_m^{(k)}(z) = \sum_{i=1}^{4} B_{kmi} e^{\lambda_{kmi} z},$$

$$W_m^{(k)}(z) = \sum_{i=1}^{4} \bar{C}_{kmi} B_{kmi} e^{\lambda_{kmi} z}. \tag{56}$$

Moreover, the coefficient $\bar{C}_{kmi}$ appearing in Eqs. (56) is determined from the following relation:

$$\bar{C}_{kmi} = \frac{\bar{C}_{44}^{(k)} \lambda_{km}^2 - \alpha_m^2 \bar{C}_{22}^{(k)}}{\alpha_m \lambda_{km} (\bar{C}_{23}^{(k)} + \bar{C}_{44}^{(k)})}. \tag{57}$$

Next, with $\alpha_m = (2m+1)\frac{\pi}{2b}$, the following Fourier sine expansion for y is used in Eqs. (48):

$$y = \sum_{m=0}^{\infty} a_m \sin(\alpha_m y), \tag{58a}$$

and:

$$a_m = \frac{8b}{\pi^2} \frac{(-1)^m}{(2m+1)^2}. \tag{58b}$$

Thus, the displacement components within the kth layer of the laminate are given by:

$$u_1^{(k)}(x,y,z) = -\frac{\bar{B}_{11}}{\bar{A}_{11}\bar{D}_{11} - \bar{B}_{11}^2} \frac{M_0}{2b} x,$$

$$u_2^{(k)}(x,y,z) = \sum_{m=1}^{\infty} B_{km} \sin(\alpha_m y) + E_k z + F_k + \sum_{m=0}^{\infty} \sum_{i=1}^{4} B_{kmi} e^{\lambda_{kmi} z} \sin(\alpha_m y),$$

$$u_3^{(k)}(x,y,z) = \sum_{m=0}^{\infty} + \sum_{i=1}^{4} \bar{C}_{kmi} B_{kmi} e^{\lambda_{kmi} z} \cos(\alpha_m y), \tag{59}$$

where:

$$B_{km} = \frac{\bar{C}_{12}^{(k)}}{\bar{C}_{22}^{(k)}} \frac{\bar{B}_{11}}{\bar{A}_{11}\bar{D}_{11} - \bar{B}_{11}^2} \frac{M_0}{2b} a_m. \tag{60}$$

It is to be noted that the constant F_k being in Eqs. (59) is a part of the rigid body translations and can, therefore, be ignored. The remaining unknown constants in Eqs. (59) (i.e., B_{kmi} and E_k) are obtained by imposing the traction-free boundary conditions at the top and bottom surface of the laminate, and the displacement continuity conditions and the stress equilibrium conditions at the interfaces. For completeness, these conditions are listed here:

The traction-free conditions at the top surface of the first layer (i.e. $\sigma_z^{(1)} = \sigma_{yz}^{(1)} = 0$):

$$\bar{C}_{23}^{(1)} u_{2,y}^{(1)} + \bar{C}_{33}^{(1)} u_{3,z}^{(1)} = \bar{C}_{13}^{(1)} \bar{L},$$

$$\bar{C}_{44}^{(1)} (u_{2,z}^{(1)} + u_{3,y}^{(1)}) = 0. \tag{61a}$$

The traction-free conditions at the bottom surface of the Nth layer (i.e. $\sigma_z^{(N)} = \sigma_{yz}^{(N)} = 0$):

$$\bar{C}_{23}^{(N)} u_{2,y}^{(N)} + \bar{C}_{33}^{(N)} u_{3,z}^{(N)} = -\bar{C}_{13}^{(N)} \bar{L},$$

$$\bar{C}_{44}^{(N)} (u_{2,z}^{(N)} + u_{3,y}^{(N)}) = 0. \tag{61b}$$

The displacement continuity conditions at the kth interface:

$$u_2^{(k)} = u_2^{(k+1)}, \quad \text{and} \quad u_3^{(k)} = u_3^{(k+1)}. \tag{61c}$$

The stress equilibrium conditions at the kth interface (i.e. $\sigma_z^{(k)} = \sigma_z^{(k+1)}$ and $\sigma_{yz}^{(k)} = \sigma_{yz}^{(k+1)}$):

$$\bar{C}_{23}^{(k)} u_{2,y}^{(k)} + \bar{C}_{33}^{(k)} u_{3,z}^{(k)} + \bar{C}_{13}^{(k)} \bar{L} = \bar{C}_{23}^{(k)} u_{2,y}^{(k+1)} + \bar{C}_{33}^{(k+1)} u_{3,z}^{(k+1)} \bar{L},$$

$$\bar{C}_{44}^{(k)} (u_{2,z}^{(k)} + u_{3,y}^{(k)}) = \bar{C}_{44}^{(k+1)} (u_{2,z}^{(k+1)} + u_{3,y}^{(k+1)}). \tag{61d}$$

In order to be able to impose the conditions stated before, the parameter, $\bar{L}$, appearing in Eqs. (61) can be expended in the Fourier cosine series as:

$$\bar{L} = \sum_{M=0}^{\infty} \bar{L} b_m \cos(\alpha_m y), \tag{62a}$$

where $\alpha_m = (2m+1)\frac{\pi}{2b}$ and:

$$b_m = \frac{4}{\pi} \frac{(-1)^m}{2m+1}. \tag{62b}$$

For a general cross-ply laminate with N layers, substituting Eqs. (59) and (62a) into Eqs. (61) generates $4N$ algebraic equations, which, upon solving, will produce the $4N$ unknown constants of integrations, B_{kmi}, appearing in Eqs. (59) for each Fourier integer, m. The remaining unknown constant (i.e., E_k) will be obtained to be equal to zero. As a result, the strain and stress components will readily be determined from the strain-displacement relations in Eqs. (11) and the Hooke law in Eq. (12), respectively.

It is noted that the elasticity solution presented here is an analytical solution and not an exact solution because of the Gibbs phenomenon in the Fourier expansions introduced in Eqs. (58a) and (62a). In fact, according to the solution found here, the interlaminar normal stress, σ_z, will vanish at points located on the edges of the laminate at $y = \pm b$. This is, of course, not a correct result, since an exact elasticity solution would yield nonzero values for σ_z on theses edges. The exact value of σ_z on these edges, however, is determined by considering the following three-dimensional Hooke's law [31]:

$$\varepsilon_x^{(k)} = \bar{S}_{11}^{(k)} \sigma_x^{(k)} + \bar{S}_{12}^{(k)} \sigma_y^{(k)} + \bar{S}_{13}^{(k)} \sigma_z^{(k)},$$

$$\varepsilon_z^{(k)} = \bar{S}_{13}^{(k)} \sigma_x^{(k)} + \bar{S}_{23}^{(k)} \sigma_y^{(k)} + \bar{S}_{33}^{(k)} \sigma_z^{(k)}, \tag{63}$$

where $\bar{S}_{ij}^{(k)}$'s are the transformed compliances of the kth layer. At the edges of the laminate, $u_3^{(k)}$ is specified to vanish (see Eq. (39)). Therefore, at all points on these edges (expect for points located at the intersections of these edges with interfaces, bottom surface, and top surface of the laminate), the following result can be concluded:

$$\varepsilon_z = \frac{\partial u_3^{(k)}}{\partial z} = 0 \quad \text{at} \quad y = \pm b. \tag{64}$$

Next, it is noted that the substitution of Eqs. (38) and (64) into Eqs. (63) results in:

$$\bar{L} = \bar{S}_{11}^{(k)} \sigma_x^{(k)} + \bar{S}_{13}^{(k)} \sigma_z^{(k)}, \tag{65a}$$

$$0 = \bar{S}_{13}^{(k)} \sigma_x^{(k)} + \bar{S}_{33}^{(k)} \sigma_z^{(k)}. \tag{65b}$$

Solving Eqs. (65) yields the exact value of $\sigma_z^{(k)}$, found to be as:

$$\sigma_z^{(k)} = \frac{\bar{S}_{13}^{(k)} \bar{L}}{\bar{S}_{13}^{(k)2} - \bar{S}_{11}^{(k)} \bar{S}_{33}^{(k)}}, \tag{66}$$

where $\bar{L} = -\frac{\bar{B}_{11}}{\bar{A}_{11}\bar{D}_{11} - \bar{B}_{11}^2} \frac{M_0}{2b}$. This relation marks that the interlaminar normal stress has a constant value at the edges of each lamina and that, furthermore, this constant value becomes different from one layer to another (adjacent) layer because of changes in fiber direction.

4. Numerical results and discussions

In this section, several numerical examples are accessible for general cross-ply laminates under the bending moment, M_0. The on-axis mechanical properties of each ply are taken to be those of graphite/epoxy T300/5208, as given in [31]:

$$E_1 = 132\text{GPa}, \qquad E_2 = E_3 = 10.8\text{GPa},$$

$$G_{12} = G_{13} = 5.65\text{GPa}, \quad G_{23} = 3.38\text{GPa},$$

$$\nu_{12} = \nu_{13} = 0.24, \qquad \nu_{23} = 0.59. \tag{67}$$

In addition, the thickness of each ply is assumed to be 0.5 mm and the value 5/6 is used for the shear correction factor, k_4^2, in the FSDT. All the numerical results shown in what follows are presented by means of the following normalized:

$$\bar{B}_j = \frac{B_j}{M_0} \quad (j = 2.6), \tag{68}$$

$$\bar{\sigma}_{ij} = \frac{\sigma_{ij}}{\sigma_0}, \tag{69}$$

where $\sigma_0 = \frac{M_0}{bh^2}$. Also, for obtaining accurate results within LWT, each physical lamina is divided into, unless otherwise mentioned, 12 sublayers (i.e., $p = 12$).

Table 1. Numerical values of $\bar{B}_6$ for various laminates according to FSDT and LWT.

Laminate	Theory	$2b/h=5$	$2b/h=10$	$2b/h=20$
[90°/90°/90°/0°]	FSDT	0.9725	0.4863	0.2431
	LWT	0.9172	0.4590	0.2292
[0°/0°/0°/90°]	FSDT	0.6744	0.3372	0.1668
	LWT	0.6494	0.3250	0.1625
[90°/90°/0°/0°]	FSDT	0.8514	0.4257	0.2129
	LWT	0.8110	0.4056	0.2027
[90°/0°/90°/90°]	FSDT	1.2196	0.6098	0.3049
	LWT	1.1553	0.5775	0.2884

To closely study the accuracy of FSDT in estimating B_6, numerical results for ratio $\bar{B}_6$, according to FSDT and LWT, are obtained and presented in Table 1 for different width to thickness ratios and various general cross-ply laminates. Close agreements are seen to exist between the results of the two theories, particularly for thin to moderately thick laminates. Numerical study indicates that the terms involving B_6 in Eqs. (25) have unimportant effects on distribution of interlaminar stress within various laminates, even for thick laminate. It is, therefore, concluded here that the formula obtained for B_6, according to FSDT, may always be utilized for various cross-ply laminates under bending within other theories, such as LWT and elasticity theory (see Eq. (14)).

Next, in order to assess the accuracy of LWT, the results of LWT are compared here with those of elasticity solutions as developed in the present study for loading case 2 (see Eq. (24) and the boundary conditions in Eq. (39)). The boundary conditions used in LWT, equivalent to those in the elasticity solution (see Eq. (39)), are as:

$$M_y^k = W_k = 0 \quad \text{at} \quad y = \pm b. \tag{70}$$

The interlaminar stresses, $\sigma_z^{(k)}$ and $\sigma_{yz}^{(k)}$, are calculated in LWT by integrating the local elasticity equations of equilibrium. In order to find the correct value of interlaminar normal stress within LWT at exactly $y = \pm b$, a procedure similar to that undertaken here within the elasticity solution is employed. Toward this goal, it is noted that by using the boundary conditions (Eq. (70)) in the laminate constitutive relations (Eqs. (31)), the following relation is achieved:

$$D_{22}^{kj} V_j' = -B_{12}^k \bar{L} \quad \text{at} \quad y = \pm b. \tag{71}$$

Quantity V_j at $y = \pm b$ is obtained from Eq. (71). Next, upon substitution of this quantity into the strain-displacement relations in Eqs. (28) and the subsequent results into Eq. (12), interlaminar normal stress, σ_z, is obtained within LWT at the edges of the laminate.

In what follows, numerical results are developed for various general cross-ply laminates with free edges only, and with width to thickness ratio (i.e., 2b/h) equal to 5, according to LWT. Both loading cases defined in Eqs. (23) and (24) will be considered. Figures 2 to 4 show the distribution of interlaminar normal and shear stresses along the width of [0°/ 90°/ 0°/ 90°], [90°/ 90°/ 90°/ 0°] and [90°/ 0°/ 90°/ 0°] laminates, respectively.

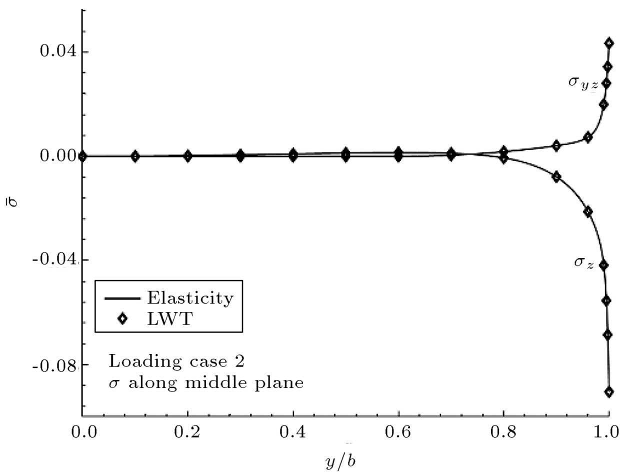

Figure 2. Distribution of interlaminar stresses along the middle plane of [0°/ 90°/ 0°/ 90°] laminate.

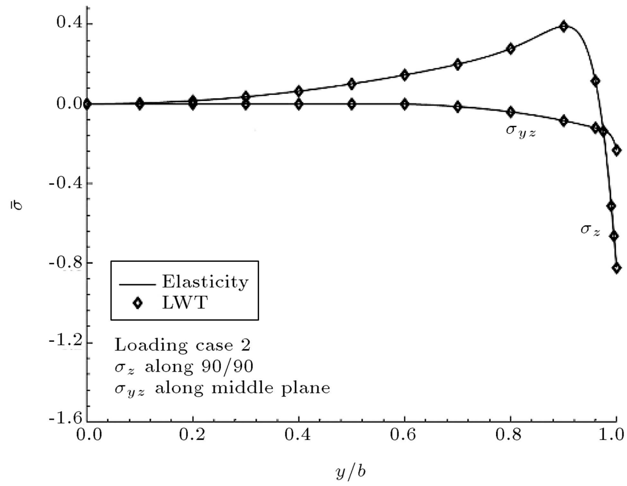

Figure 3. Distribution of interlaminar stresses along the 90°/ 90° interface and middle plane of [90°/90°/90°/0°] laminate.

Excellent agreement between the layerwise solution and the elasticity solution is seen. This close agreement verifies the accuracy of the LWT. It is reminded that these results are obtained for loading case 2. To study the convergence of the stresses near free edges, two simple laminates, [0°/ 90°/ 0°/ 90°] and [0°/ 90°/ 90°/ 0°], subjected to the bending moment, M_0, are considered. Since, except exactly at $y = b$, the difference in σ_z with various p at the laminate interfaces and through the thickness in the boundary-layer region is small, the value of σ_x at $y = b$ is used in the convergence study. Figure 5 shows the numerical value of σ_z at exactly $y = b$ versus p for both [0°/ 90°/ 90°/ 0°] and [0°/ 90°/ 90°/ 0°] laminates for loading case 1. At the unsymmetric laminate, [0°/ 90°/ 90°/ 0°], (the grid line in Figure 5), it is seen that the numerical value of σ_z is more noticeably dependent on the number of subdivisions, p, than the symmetric laminate, [0°/ 90°/ 90°/ 0°]. At the symmetric laminate the numerical value of σ_z is seen to remain constant with the increasing number of numerical layers (for $p > 9$) but at the unsymmetric laminate it is seen to remain constant (for $p > 12$). The distribution of interlaminar normal stress, σ_z, along the lower interfaces (0°/ 90° and 90°/ 0°), of [0°/ 0°/ 0°/ 90°], and [90°/ 90°/ 90°/ 0°], laminates, respectively, for loading case 1, is exhibited in Figure 6. The figure demonstrates that in the boundary-layer region, σ_z first becomes negative and then positive for [0°/ 0°/ 0°/ 90°] laminate, and for [90°/ 90°/ 90°/ 0°] laminate, σ_z is negative totally. However, the magnitude of σ_z becomes quite large for two laminates. Figure 7 displays the distribution of

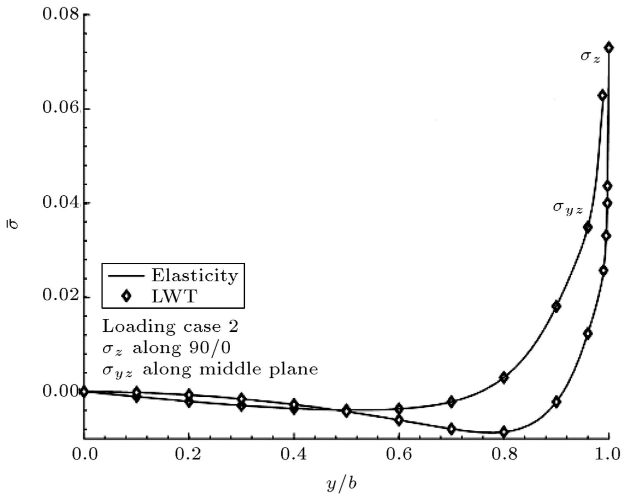

Figure 4. Interlaminar stresses along the 90°/ 0° interface and middle plane of [90°/0°/90°/0°] laminate.

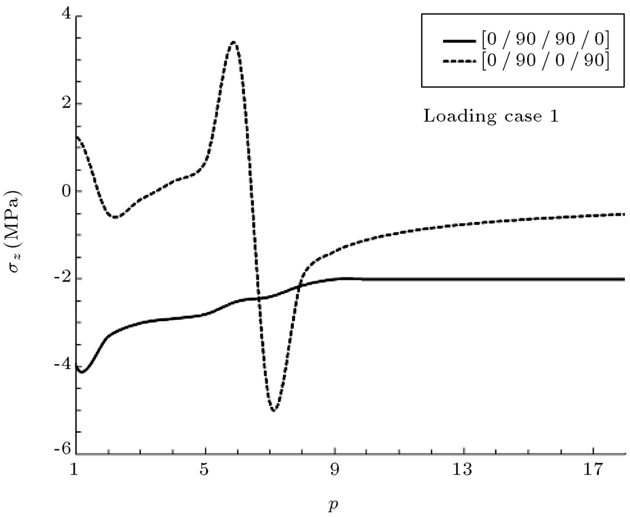

Figure 5. Convergence of interlaminar normal stress σ_z at $y = b$ at middle plane in [0°/ 90°/ 0°/ 90°] and [0°/ 90°/ 90°/ 0°] laminates under the bending moment versus the number of layer subdivisions (p).

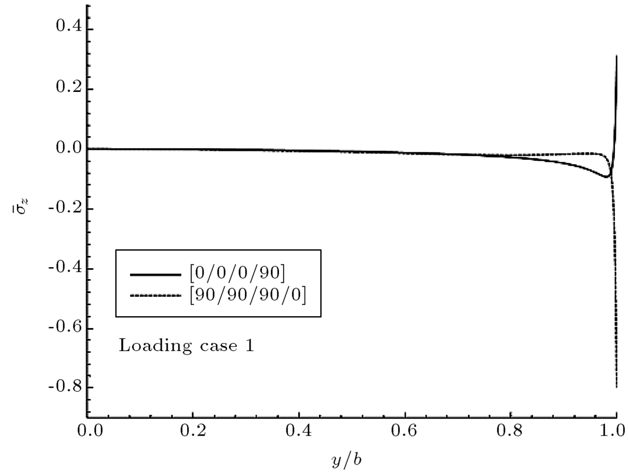

Figure 6. Distribution of interlaminar normal stress $\bar{\sigma}_z$ along the 0°/ 90°and 90°/ 0° interfaces of [0°/ 0°/ 0°/ 90°] and [90°/ 90°/ 90°/ 0°] laminates, respectively.

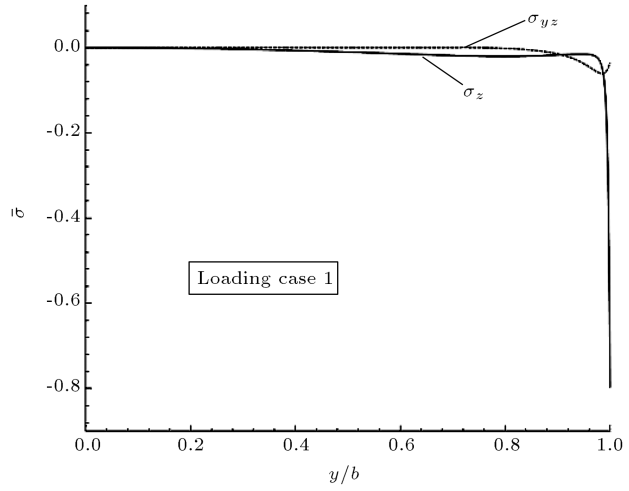

Figure 7. Interlaminar stresses along the 90°/ 0° interface of [90°/ 90°/ 90°/ 0°] laminate.

the interlaminar stresses along the 90°/ 0° interface of [90°/ 90°/ 90°/ 0°] laminate for loading case 1. It is observed that the interlaminar normal stress, σ_z, grows rapidly in the vicinity of the free edges, while is zero in the interior region of the laminate. On the other hand, σ_{yz} rises toward the free edge and decreases rather abruptly to zero at the free edge. It is also seen that the magnitude of the maximum of the transverse normal stress, σ_{yz}, is greater than that of transverse shear stress. By raising the number of numerical layers in each lamina, σ_{yz} becomes slightly closer to zero, but, may never become zero.

This is, most likely, due to the fact that within LWT, the generalized stress resultant, R_y^k, rather than σ_{yz}, is forced to disappear at the free edge (see Eqs. (38)). The distribution of the interlaminar stresses, σ_z and σ_{yz}, along the upper (0°/ 0°), middle (0°/ 90°) and lower (90°/ 90°) interfaces of unsymmetric cross-ply [0°/ 0°/ 90°/ 90°] laminate are demonstrated in Figure 8 for loading case 2. Both stresses are seen to grow rapidly near to the free edge, while being zero in the interior region of the laminate. It is to be noted that the interlaminar shear stress, σ_{xz}, is identically zero everywhere in cross-ply laminates. The distribution of interlaminar normal stress along the (90°/ 90°) interface of [0°/ 0°/ 90°/ 90°] laminate for loading case 1 is displayed in Figure 9. It is observed that increasing the number of layer subdivisions, p, has no significant effect on the numerical value of interlaminar stress, σ_z, within the boundary-layer region of the laminate, especially at the free edge (i.e., $y = b$) because of the interface-edge junction of similar layers (i.e. 90°/ 0°). It is significant to note that increasing the number of subdivisions results in no convergence for σ_z at the interface-edge junction of two unalike layers, such as (0°/ 90°), and

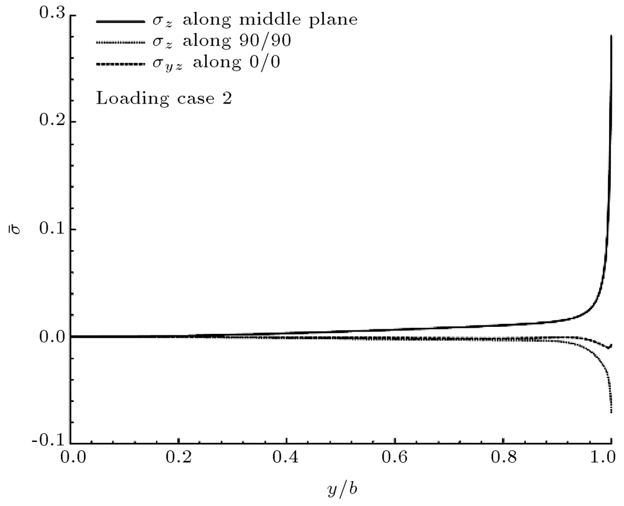

Figure 8. Distribution of interlaminar stresses along the 0°/ 0°/ 0°/ 90° and 90°/ 90° interfaces of [0°/ 0°/ 90°/ 90°] laminate.

the numerical value of this component continues to grow as the number of sublayers is increased. On the contrary, at the interface-edge junction of similar layers, such as (90°/ 90°), the numerical value of σ_z remains constant as the number of numerical layers within each physical layer is increased. Through the thickness distribution of the interlaminar normal stress, σ_z, for [90°/ 90°/ 0°/ 0°], the laminate is displayed in Figure 10 for loading case 1. It is seen that the maximum negative value of σ_z happens within the bottom 90° layer, and the maximum positive value of σ_z occurs within the top 0° layer both near the middle surface of the laminate at the free edge (i.e., $y = b$). It is also seen that σ_z diminishes away from the free edge as the interior region of the laminate is approached.

Figure 11 shows the variations of the interlaminar stress, σ_z, at $y = b$ through the thickness in the [0°/ 0°/ 0°/ 90°] laminate for loading case 2. It is seen

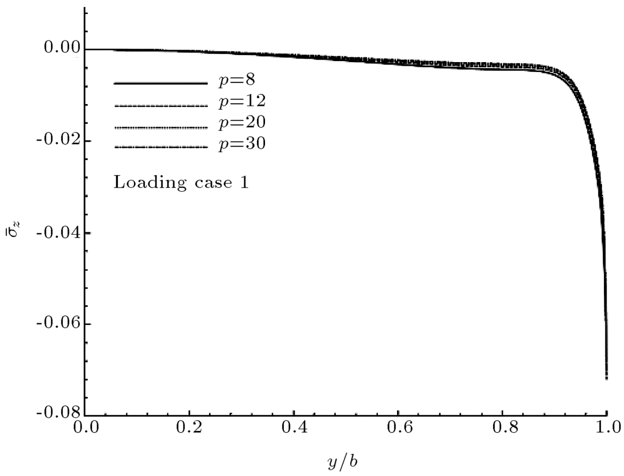

Figure 9. Distribution of interlaminar normal stress $\bar{\sigma}_z$ along the 90°/ 90° interface of [0°/ 0°/ 90°/ 90°] laminate as a function of layer subdivision number p.

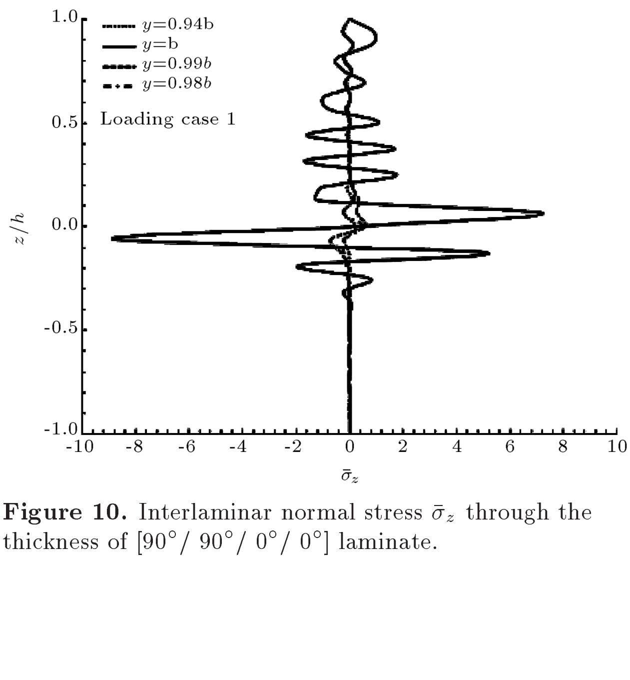

Figure 10. Interlaminar normal stress $\bar{\sigma}_z$ through the thickness of [90°/ 90°/ 0°/ 0°] laminate.

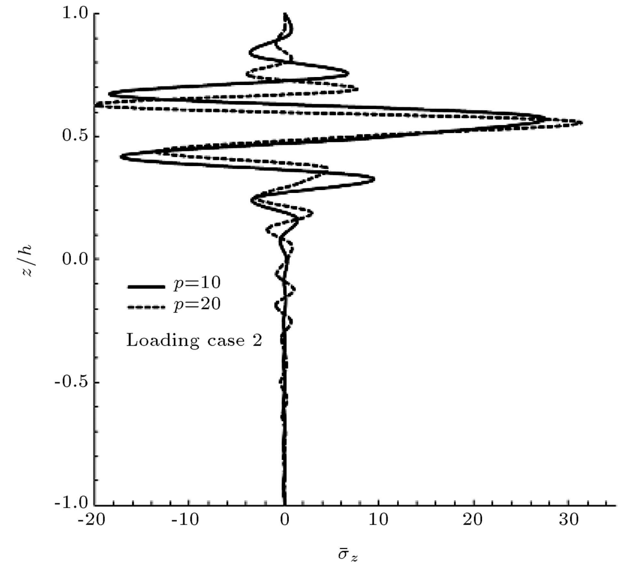

Figure 11. Distribution of interlaminar normal stress $\bar{\sigma}_z$ through the thickness of [0°/ 0°/ 0°/ 90°] laminate.

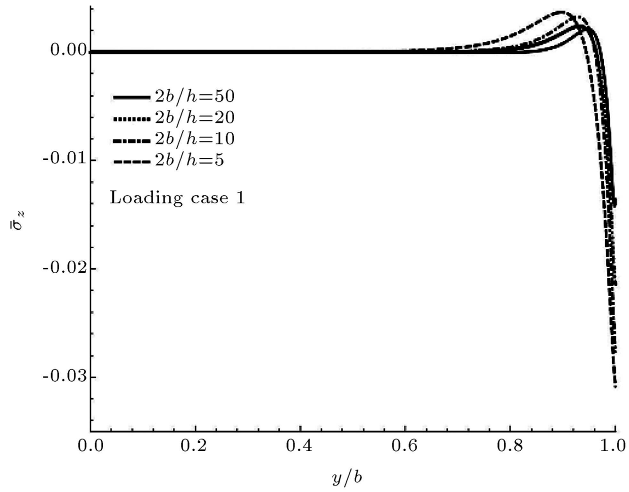

Figure 12. Interlaminar stress along the middle plane of [0°/ 90°/ 90°/ 0°] laminate for various width-to-thickness ratios.

that by increasing the number of layer subdivisions, p, the magnitude of σ_z becomes larger, especially at the interfaces.

The effect of the laminate width to thickness ratio on the interlaminar stress due to loading case 1 is examined in Figure 12 in the [0°/ 90°/ 90°/ 0°] laminate. It is seen that the width of the boundary-layer regions always remains almost equal to the thickness of the laminate. That is, a thickness away from the edges of the laminate, the interlaminar stresses approach zero.

5. Conclusions

An elasticity formulation is developed for the displacement field of a long cross-ply laminate under the bending moment. The First-order Shear Deformation Theory (FSDT) is then employed to determine the unknown constant coefficients appearing in the relevant displacement fields when the laminate is subjected to bending. Next, Reddy's layerwise theory (LWT) is utilized to examine the edge-effect interlaminar stresses. Analytical solutions to the LWT equations are obtained using the state space approach. The unknown constants, B_2 and B_6, appearing in the displacement field are also determined within LWT, and it is found that FSDT is very adequate in predicting these constants. For special boundary conditions (see Eqs. (38)), an analytical elasticity solution is developed to verify the accuracy of the layerwise theory in describing interlaminar stresses. Excellent agreement is seen to exist between the results of the LWT and those of the elasticity theory. Several numerical results according to LWT are then developed for the interlaminar stresses through the thickness and across the interfaces of the different cross-ply laminates. A convergence study is performed to determine suitable subdivisions to be used within each lamina for accurate results in LWT. It is revealed that a moderately large number of numerical layers must be employed within the laminate and, in general, this number is dependent on fiber directions and the stacking sequences of the plies within the laminate.

References

1. Pipes, R.B. and Pagano, N.J. "Interlaminar stresses in composite laminates - an approximate elasticity solution", *J. Appl. Mech.*, **41**, pp. 668-672 (1974).
2. Pagano, N.J. "On the calculation of interlaminar normal stress in composite laminate", *J. Compos. Mater.*, **8**, pp. 65-81 (1974).
3. Tang, S. and Levy, A. "A boundary layer theory-part II: Extension of laminated finite strip", *J. Compos. Mater.*, **9**, pp. 42-52 (1975).
4. Hsu, P.W. and Herakovich, C.T. "Edge effects in angle-ply composite laminates", *J. Compos. Mater.*, **11**, pp. 422-428 (1977).
5. Pipes, R.B. and Pagano, N.J. "Interlaminar stresses in composite laminates under uniform axial extension", *J. Compos. Mater.*, **4**, pp. 538-548 (1970).
6. Wang, A.S.D. and Crossman, F.W. "Some new results on edge effect in symmetric composite laminates", *J. Compos. Mater.*, **11**, pp. 92-106 (1977).
7. Whitcomb, J.D., Raju, I.S. and Goree, J.G. "Reliability of the finite element method for calculating free edge stresses in composite laminates", *Comput. Struct.*, **15**(1), pp. 23-37 (1972).
8. Kant, T. and Swaminathan, K. "Estimation of transverse interlaminar stresses in laminated composites - a selective review and survey of current developments", *Compos. Struct.*, **49**, pp. 65-75 (2000).

9. Tang, S. "Interlaminar stresses of uniformly loaded rectangular composite plates", *J. Compos. Mater.*, **10**, pp. 69-78 (1976).

10. Lo, K.H., Christensen, R.M. and Wu, E.M. "A high-order theory of plate deformation. Part 2: Laminated plates", *J. Appl. Mech.*, **44**, pp. 669-676 (1977).

11. Murthy, P.L.N. and Chamis, C.C. "Free-edge delamination: Laminate width and loading conditions effects", *J. Comp. Technol. Res.*, **11**(1), pp. 15-22 (1989).

12. Kassapoglou, C. "Determination of interlaminar stresses in composite laminates under combined loads", *J. Reinf. Plast. Compos.*, **9**(1), pp. 33-58 (1990).

13. Barbero, E.J., Reddy, J.N. and Teply, J. "An accurate determination of stresses in thick laminates using a generalized plate theory", *Int. J. Numer. Methods. Eng.*, **29**, pp. 1-14 (1990).

14. Savoia, M. and Reddy, J.N. "A variational approach to three-dimensional elasticity solutions of laminated composite plates", *J. Appl. Mech.*, **59**, pp. 166-175 (1992).

15. Wu, C-P. and Kuo, H.C. "Interlaminar stresses analysis for laminated composite plates based on a local high order lamination theory", *Compos. Struct.*, **20**, pp. 237-247 (1992).

16. Wu, C-P. and Yen, C-B. "Interlaminar stress mixed finite element analysis of unsymmetric laminated composite plates", *Comput. Struct.*, **49**(3), pp. 411-419 (1993).

17. Kim, T. and Atluri, S.N. "Interlaminar stresses in composite laminates under out-of-plane shear/bending", *AIAA J.*, **32**(8), pp. 1700- 1708 (1994).

18. Robbins, D.H. and Reddy, J.N. "Modelling of thick composites using a layerwise laminate theory", *Int. J. Numer. Methods Eng.*, **36**, pp. 655-677 (1993).

19. Lee, C.Y. and Chen, J.M. "Interlaminar shear stress analysis of composite laminate with layer reduction technique", *Int. J. Numer. Methods Eng.*, **39**, pp. 847-865 (1996).

20. Shu, X-P. and Soldatos, K.P. "Cylindrical bending of angle-ply laminates subjected to different sets of edge boundary conditions", *Int. J. Solids Struct.*, **37**, pp. 4289-4307 (2000).

21. Huang, Y., Di, S., Wu, C. and Sun, H. "Bending analysis of composite laminated plates using a partially hybrid stress element with interlaminar continuity", *Comput. Struct.*, **80**, pp. 403-410 (2002).

22. Matsunaga, H. "Assessment of a global higher-order deformation theory for laminated composite and sandwich plates", *Compos. Struct.*, **56**, pp. 279-291 (2002).

23. Mittelstedt, C. and Becker, W. "Reddy's layerwise laminate plate theory for the computation of elastic fields in the vicinity of straight free laminate edges", *Mater. Science and Eng.*, **498**, pp. 76-80 (2008).

24. Jin Na, W. "Damage analysis of laminated composite beams under bending loads using the layer-wise theory", Dissertation Thesis, Texas A&M University (2008).

25. Nosier, A. and Maleki, M. "Free edge stresses in general composite laminates", *Int. J. Mech. Sciences*, **50**, pp. 1435-47 (2008).

26. Kim, H., Lee, J. and Cho, M. "Free-edge interlaminar stress analysis of composite laminates using interface modeling", *J. Eng. Mech.*, **138**(8), pp. 973-983 (2012).

27. Lee, J., Cho, M. and Kim, H.S. "Bending analysis of a laminated composite patch considering the free-edge effect using a stress-based equivalent single-layer composite model", *Int. J. Mech. Sciences*, **53**(8), pp. 606-616 (2011).

28. Ahn, J.S., Kim, S.D., Chang, C.H., Lee, D.W. and Woo, K.S. "Prediction of free edge stresses in laminate systems using multi-dimensional method based on higher-order modeling", *Appl. Mech. and Mater.*, **105**, pp. 1260-1263 (2011).

29. Lekhnitskii, S.G., *Theory of Elasticity of an Anisotropic Body*, Mir Publishers, Moscow (1981).

30. Fung, Y.C., *Foundations of Solid Mechanics*, Prentice-Hall, Englewood Cliffs, NJ (1965).

31. Herakovich, C.T., *Mechanics of Fibrous Composites*, John Wiley & Sons, New York (1998).

32. Reddy, J.N. *Mechanics of Laminated Composite Plates and Shells: Theory and Analysis*, CRC Press, New York (2003).

33. Nosier, A., Kapania, R.K. and Reddy, J.N. "Free vibration analysis of laminated plates using a layerwise theory", *AIAA J.*, **13**(12), pp. 2335-46 (1993).

Appendix A

The constants coefficients appearing in Eq. (22) are defined as:

$$\bar{A}_{11} = A_{11} - A_{12}\bar{a}_1 - B_{12}\bar{b}_2,$$

$$\bar{B}_{11} = B_{11} - A_{12}\bar{b}_1 - B_{12}\bar{a}_2,$$

$$\bar{D}_{11} = D_{11} - B_{12}\bar{b}_1 - D_{12}\bar{a}_2, \tag{A.1}$$

where:

$$(\bar{a}_1, \bar{a}_2, \bar{b}_1, \bar{b}_2) = \frac{1}{A_{22}D_{22} - B_{22}^2}[(A_{12}D_{22} - B_{12}B_{22}),$$

$$(A_{22}D_{12} - B_{12}B_{22}), (B_{12}D_{22} - B_{22}D_{12}),$$

$$(A_{22}B_{12} - A_{12}B_{22})], \tag{A.2}$$

also:

$$(A_{ij}, B_{ij}, D_{ij}) = \int_{-h/2}^{h/2} \bar{Q}_{ij}^{(k)}(1, z, z^2)dz, \tag{A.3}$$

are the rigidities in the first-order shear deformation theory and $\bar{Q}_{ij}^{(k)}$'s are the transformed (i.e., off-axis) reduced stiffnesses of the kth layer.

Appendix B

The laminate rigidities, being in Eqs. (32), upon integration, are presented in the following form:

$$(A_{pq}^{kj}, B_{pq}^{kj}, D_{pq}^{kj}) = \begin{cases} \left(-\frac{\bar{C}_{pq}^{(k-1)}}{h_{k-1}}, !\frac{\bar{C}_{pq}^{(k-1)}}{2}, \frac{h_{k-1}\bar{C}_{pq}^{(k-1)}}{6}\right) & \text{if } j = k-1 \\ \left(\frac{\bar{C}_{pq}^{(k-1)}}{h_{k-1}}, +\frac{\bar{C}_{pq}^{(k)}}{h_k}, \frac{\bar{C}_{pq}^{(k-1)}}{2} - \frac{\bar{C}_{pq}^{(k)}}{2}, \frac{h_{k-1}\bar{C}_{pq}^{(k-1)}}{3}, +\frac{h_k\bar{C}_{pq}^{(k)}}{3}\right) & \text{if } j = k \\ \left(-\frac{\bar{C}_{pq}^{(k)}}{h_k}, \frac{\bar{C}_{pq}^{(k)}}{2}, \frac{h_k\bar{C}_{pq}^{(k)}}{6}\right) & \text{if } j = k+1 \\ (0,0,0) & \text{if } j<k-1 \text{ or } j>k+1 \end{cases} \tag{B.1}$$

and:

$$(A_{pq}^{k}, B_{pq}^{k}, \bar{B}_{pq}^{k}, D_{pq}^{k}) = \begin{cases} \left(-\bar{C}_{pq}^{(1)}, \frac{h_1\bar{C}_{pq}^{(1)}}{2}, \bar{C}_{pq}^{(1)}\frac{z_1^2-z_2^2}{2h_1}, \frac{\bar{C}_{pq}^{(1)}}{h_1}\left[\frac{z_1^3-z_2^3}{3} - z_2\frac{z_1^2-z_2^2}{2}\right]\right) & \text{if } k=1 \\ \left(-\bar{C}_{pq}^{(k-1)}, \frac{h_{k-1}\bar{C}_{pq}^{(k-1)}}{2}, \bar{C}_{pq}^{(k-1)}\frac{z_k^2-z_{k-1}^2}{2h_{k-1}}, \frac{\bar{C}_{pq}^{(k-1)}}{h_{k-1}}\left[\frac{z_k^3-z_{k-1}^3}{3} - z_{k-1}\frac{z_k^2-z_{k-1}^2}{2}\right]\right) & \text{if } k=N+1 \\ \left(\bar{C}_{pq}^{(k-1)} - \bar{C}_{pq}^{(k)}, \frac{h_{k-1}\bar{C}_{pq}^{(k-1)}}{2} + \frac{h_k\bar{C}_{pq}^{(k)}}{2}, \bar{C}_{pq}^{(k-1)}\frac{z_k^2-z_{k-1}^2}{2h_{k-1}} + \bar{C}_{pq}^{(k)}\frac{z_k^2-z_{k-1}^2}{2h_k}, \frac{\bar{C}_{pq}^{(k-1)}}{h_{k-1}}\left[\frac{z_k^3-z_{k-1}^3}{3} - z_{k-1}\frac{z_k^2-z_{k-1}^2}{2}\right] + \frac{\bar{C}_{pq}^{(k)}}{h_k}\left[\frac{z_k^3-z_{k+1}^3}{3} - z_{k-1}\frac{z_k^2-z_{k+1}^2}{2}\right]\right) & \text{if } 1<k<N+1 \end{cases} \tag{B.2}$$

also:

$$(A_{pq}, B_{pq}, D_{pq}) = \sum_{i=1}^{N} \bar{C}_{pq}^{(i)} \times \left([Z_{i+1} - Z_i], \left[\frac{z_{i+1}^2 - Z_i^2}{2}\right], \left[\frac{Z_{i+1}^3 - Z_i^3}{3}\right]\right). \tag{B.3}$$

The coefficient matrices $[M]$, $[K]$, and $[T]$ appearing in Eq. (35) are given as:

$$[M] = \begin{bmatrix} [D_{22}] & [B_{23}] - [B]_{44}^T \\ [0] & [D_{44}] \end{bmatrix},$$

$$[K] = \begin{bmatrix} -([A_{44}] + [\alpha]) & [0] \\ [B_{44}] - [B_{23}]^T & -([A_{33}] + [\alpha]) \end{bmatrix},$$

$$[T] = \begin{bmatrix} \{0\} & \{0\} \\ \{A_{13}\} & \{B_{13}\} \end{bmatrix}, \tag{B.4}$$

where $[A_{pq}], [B_{pq}]$ and $[D_{pq}]$ are $(N+1)\times(N+1)$ square matrices containing A_{pq}^{kj}, B_{Pq}^{kj}, and D_{pq}^{kj} respectively, and the vectors, $\{A_{pq}\}, \{B_{pq}\}$, and $\{\bar{B}_{pq}\}$, are $(N+1)\times 1$ column matrices containing A_{pq}^{k}, B_{pq}^{k}, and $\bar{B}_{pq}^{k}$ respectively. Also, $[0]$ is $(N+1)\times(N+1)$ square zero and $\{0\}$ is a zero vector with $N+1$ rows. The artificial matrix, $[\alpha]$, is also a $(N+1)\times(N+1)$ square matrix, whose elements are given by:

$$\alpha^{kj} = \alpha \int_{-h/2}^{h/2} \phi_k \phi_j dz, \tag{B.5}$$

with α being a relatively small parameter in comparison with the rigidity constants, $A_{pq}^{kj} (pq = 33, 44, 55)$. It is to be noted that the inclusion of $[\alpha]$ in matrix $[K]$ makes the eigenvalues of matrix $(-[M]^{-1}[K])$ be all distinct.

Biography

Hamidreza Yazdani Sarvestani obtained a BS degree from Shiraz University, Iran, an MS degree in Applied Mechanics and Design from Sharif University of Technology, Tehran, Iran, and is currently a PhD degree student in the Department of Mechanical and Industrial Engineering at Concordia University at Canada. His research interests include stress analysis and design of composite structures.